B-1.3. Studies on formation and loss processes of SO_3 for a model including aerosol production

Contact person Takashi Imamura
Head
Ozone Layer Research Team
Global Environmental Research Group
National Institute for Environmental Studies
Environment Agency
16-2 Onogawa, Tsukuba, Ibaraki 305-0053, Japan
Phone: +81-298-50-2406, Fax: +81-298-50-2579
E-mail: imamura@nies.go.jp

Total Budget for FY1997 - FY1999 31,625,000 Yen (FY1999: 10,492,000 Yen)

Abstract Two types of experiments have been performed; i.e., rate measurements of the elementary processes and chamber experiments, to elucidate the mechanisms and to quantify the efficiencies of the photooxidation of reduced sulfur compounds.

Rates of oxidation reactions of SO, CH_3S, and HS radicals by peroxy radicals were measured for the first time by means of time-resolved photoionization mass spectrometry combined with pulsed-laser photolysis. It was found that all of the radicals investigated in this project could react with CH_3O_2 radicals rapidly with rate constant of ca. 10^{-10} $cm^3molecule^{-1}s^{-1}$. This suggests that peroxy radicals can promote the oxidation of these sulfur-containing radicals.

The yield of SO_2 formation from the photooxidation of CH_3SCH_3 was measured as a function of the NO_x concentration and temperature. It was found that the SO_2 yield increased with increasing temperature and with decreasing the concentration of NO_x. The experimental results could be explained in terms of the temperature dependent reactions of CH_3SO_2.

Key Words Reduced sulfur compound, Oxidation process, Peroxy radical, reaction rate constant, SO_2 formation yield

1. Introduction

Aerosols in the atmosphere scatter a significant fraction of incoming solar radiation back to space and lead to a cooling of the Earth's system. They also absorb terrestial radiation and contribute to a heating of the system. Aerosols also serve as cloud condensation nuclei and must affect the albedo of clouds. Hence, the changes in the abundance of aerosols could lead to a significant effect on radiative forcing. However, the impact of aerosols on forcing still is not quantified as pointed in the IPCC report (1996). [1]

Sulfate aerosols are one of important aerosols and are produced by the oxidation of SO_2 in the atmosphere. SO_2 is known to enter the atmosphere not only by direct emissions from volcanic and anthropogenic sources but also by the oxidation of reduced sulfur compounds, such as H_2S, CH_3SCH_3, OCS, and CS_2. However, their source strengths have not yet well-known; especially the conversion efficiencies from the reduced sulfur compounds to SO_2 have yet been

poorly quantified.

In this research project, two types of studies have been carried out to elucidate the mechanisms and quantify the efficiencies of the oxidation of sulfur compounds: rate measurements of elementary processes in the photooxidation of sulfur compounds and chamber experiments on the formation yield of SO_2 from CH_3SCH_3.

2. Oxidation of sulfur-containing radicals by peroxy radicals

2.1. Introduction

SO, CH_3S, and HS radicals are formed in the photooxidation of CH_3SCH_3 and H_2S which are dominant reduced sulfur compounds. These radicals slowly or merely react with molecular oxygen which is one of most abundant chemical constitutes of the Earth's atmosphere. Therefore, the reactions with trace gases, such as O_3 and NO_X, are important for the fate of these radicals. If the concentrations of O_3 and NO_X are low, the reactions with peroxy radicals (RO_2) would become important. However, no kinetic data on oxidation reactions of sulfur-containing radicals (R_S) by RO_2 are available. In this research project, we measured the rate constants for the following reactions to understand how fast R_S can be oxided by RO_2:

$$SO + CH_3O_2 \rightarrow SO_2 + CH_3O, \quad (1)$$

$$CH_3S + CH_3O_2 \rightarrow CH_3SO + CH_3O, \quad (2)$$

$$HS + CH_3O_2 \rightarrow HSO + CH_3O. \quad (3)$$

2.2. Experimental

Experiments were carried out by means of time-resolved photoionization mass spectrometry combined with pulsed-laser photolysis. A gas mixture of precursor molecules of CH_3O_2 and sulfur-containing radicals, R_S, diluted in carrier gas was introduced into a Pyrex glass flow reactor. An ArF excimer laser was directed along the axis of the reactor to generate radicals. Part of the reacting gas in the reactor was sampled through a pinhole (i.d. = 0.3 mm) on the wall of the reactor, and the time dependence of the radical concentration was monitored by photoionization mass spectrometry. Rate measurements were performed under the pseudo-first-order condition of $[R_S] \ll [CH_3O_2]$.

2.2.1. Formation and Detection of S-radicals

SO, CH_3S, and HS radicals were produced by laser photolysis (193 nm) of their precursor molecules as follows:

$$SO_2 + h\nu \rightarrow SO + O, \quad (4)$$

$$CH_3SCH_3 + h\nu \rightarrow CH_3S + CH_3, \quad (5)$$

$$H_2S + h\nu \rightarrow HS + H. \quad (6)$$

The radicals produced were photoionized with a Kr resonance lamp (10.0 and 10.6 eV) and detected as parent ions, such as SO^+, CH_3S^+, and HS^+.

2.2.2. Detection sensitivity of CH_3O_2

To determine the reaction rate constants, the absolute concentration of CH_3O_2 radical has to be determined or estimated. In this work, the absolute concentration was obtained using the detection sensitivity of $CH_3O_2^+$ ion signals, S_{CH3O2}:

$$[CH_3O_2] = I_{CH3O2} / S_{CH3O2}$$

where I_{CH3O2} is the intensity of the observed ion signal of $CH_3O_2^+$.

CH_3O_2 radicals were produced by the photolysis of acetone, $(CH_3)_2CO$, at 193

nm in the presence of O_2.

$$(CH_3)_2CO + h\nu \rightarrow 2\ CH_3 + CO \qquad (7)$$

$$CH_3 + O_2 + M \rightarrow CH_3O_2 + M \qquad (8)$$

CH_3O_2 radicals were photoionized with the Kr lamp and detected as $CH_3O_2^+$ ion (m/e = 47). Fig. 1a shows the timeprofile of CH_3 radicals generated in the O_2 buffer. When NO was added into the reaction system, CH_3O_2 radicals was consumed by the reaction with NO and NO_2 was produced.

$$CH_3O_2 + NO \rightarrow CH_3O + NO_2 \qquad (9)$$

Figs. 1b and c show the time profiles of CH_3O_2 and NO_2 observed in the presence of NO (5.8mTorr), respectively. The absolute concentration of CH_3O_2 consumed by reaction (9) must be equal to that of NO_2 produced. Hence, the detection sensitivity of CH_3O_2 was obtained by

$$S_{CH3O2} = I_{CH3O2}/[CH_3O_2] = I_{CH3O2}/[NO_2] = S_{NO2}\times(I_{CH3O2}/I_{NO2})$$

where I_{CH3O2} and I_{NO2} are the signal intensities of $CH_3O_2^+$ and NO_2^+ ions observed before and after introducing NO into the system, respectively. S_{NO2} represents the detection sensitivity of NO_2, which was obtained by flowing the known amount of NO_2 in the reactor.

2.3. Results and discussion

2.3.1. $SO+CH_3O_2 \rightarrow SO_2 + CH_3O$ reaction

The time dependence of relative concentration of SO radicals was measured by monitoring SO^+ ion (m/e = 48) signals. Since CH_3O_2H (m/e = 48), which produces as a secondary products in the photolysis system of acetone, interfered the profile of SO^+ signal, we measured the rate constants for the reactions of SO with CD_3O_2 using acetone-d_6. Figs. 2a and b show the time profiles of SO measured in the absence of and in the presence of CD_3O_2, respetively. Each profile could be fitted using a single exponential function and the first-order rate constant of SO, k', was obtained. Fig. 2c shows the time profile of CD_3O_2 observed simultaneously with the SO decay measurement shown in Fig. 2b. As seen in the Figure, the concentration of CD_3O_2 was almost constant during the measurement. The correction for the loss of CD_3O_2 did not need to estimate the effective concentration of CD_3O_2 during the measurement time.

Fig. 3 shows a plot of k' against the concentration of CD_3O_2 measured at the total pressure of 5 Torr. From the slope of the plot, the second-order rate constant for reaction (1), k_1, at 5 Torr was determined to be 5.9×10^{-11} $cm^3molecule^{-1}s^{-1}$. No apparent pressure dependence on k_1 was observed in the pressure range between 3 and 7 Torr. This suggests that reaction (1) is a bimolecular process. The rate constant for reaction (1) was determined to be 6×10^{-11} $cm^3molecule^{-1}s^{-1}$ by averaging the data taken at 3-7 Torr.

2.3.2. $CH_3S + CH_3O_2 \rightarrow CH_3SO + CH_3O$ reaction

The time-resolved mass spectrum of the products formed by the 193 nm photolysis of CH_3SCH_3, DMS, was observed with the Kr lamp and is shown in Fig. 4a. N_2 was used as carrier gas. The spectrum was obtained by subtracting ion signals taken for 2 ms before photolysis laser pulse from those taken during 2-4 ms after photolysis. As seen in the spectrum, CH_3 and CH_3S radicals were produced by the photolysis of DMS.

When the buffer gas was changed from N_2 to O_2, the CH_3S signal was observed with almost same intensity while the CH_3 disappeared due to reaction (8) as shown in Fig. 4b. This means that CH_3S radicals hardly react with O_2.

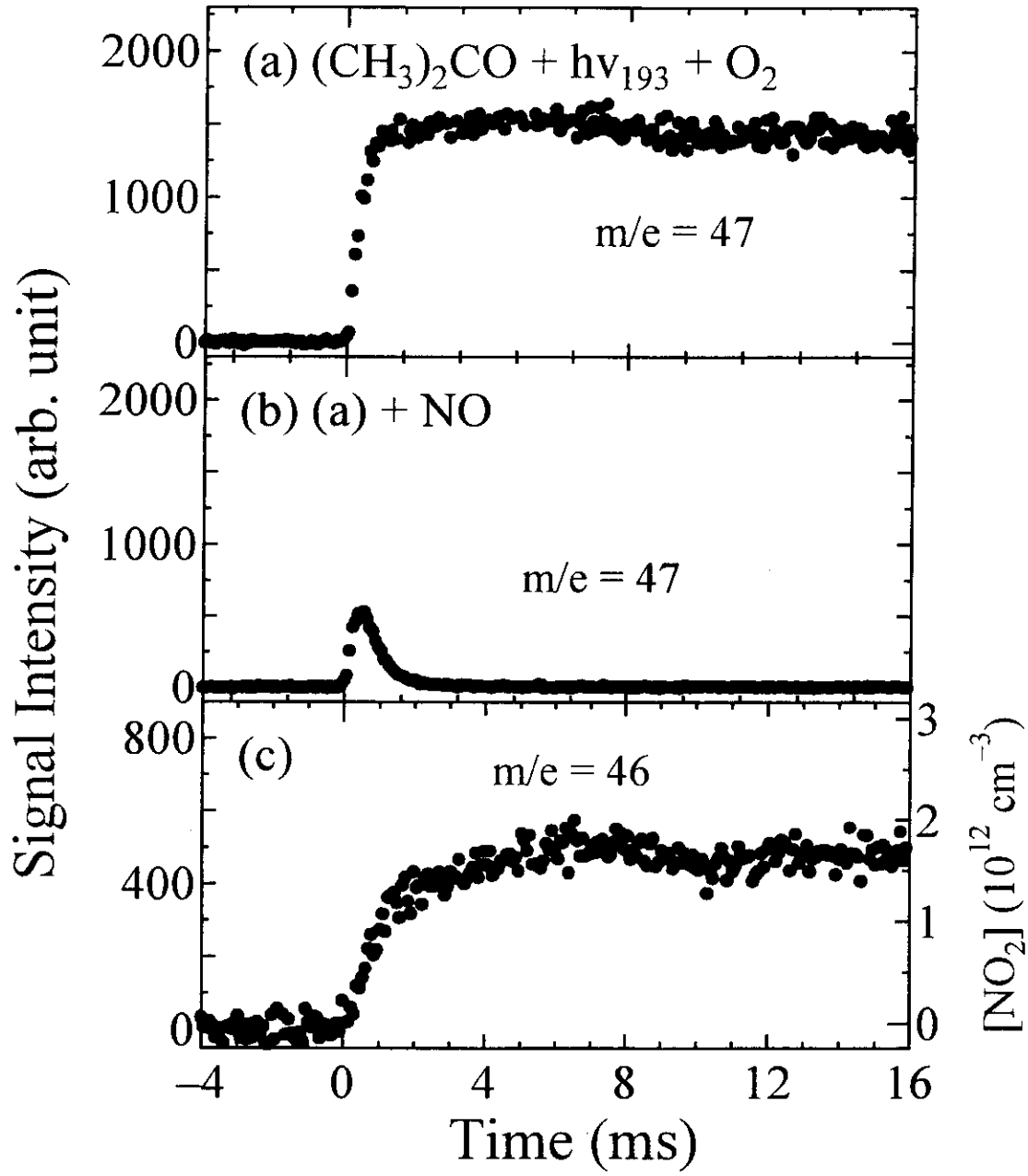

Figure 1. (a) Time profile of CH_3O_2 radicals taken in the absence of NO. Time profiles of (b) CH_3O_2 and (c) NO_2 taken in the presence of NO.

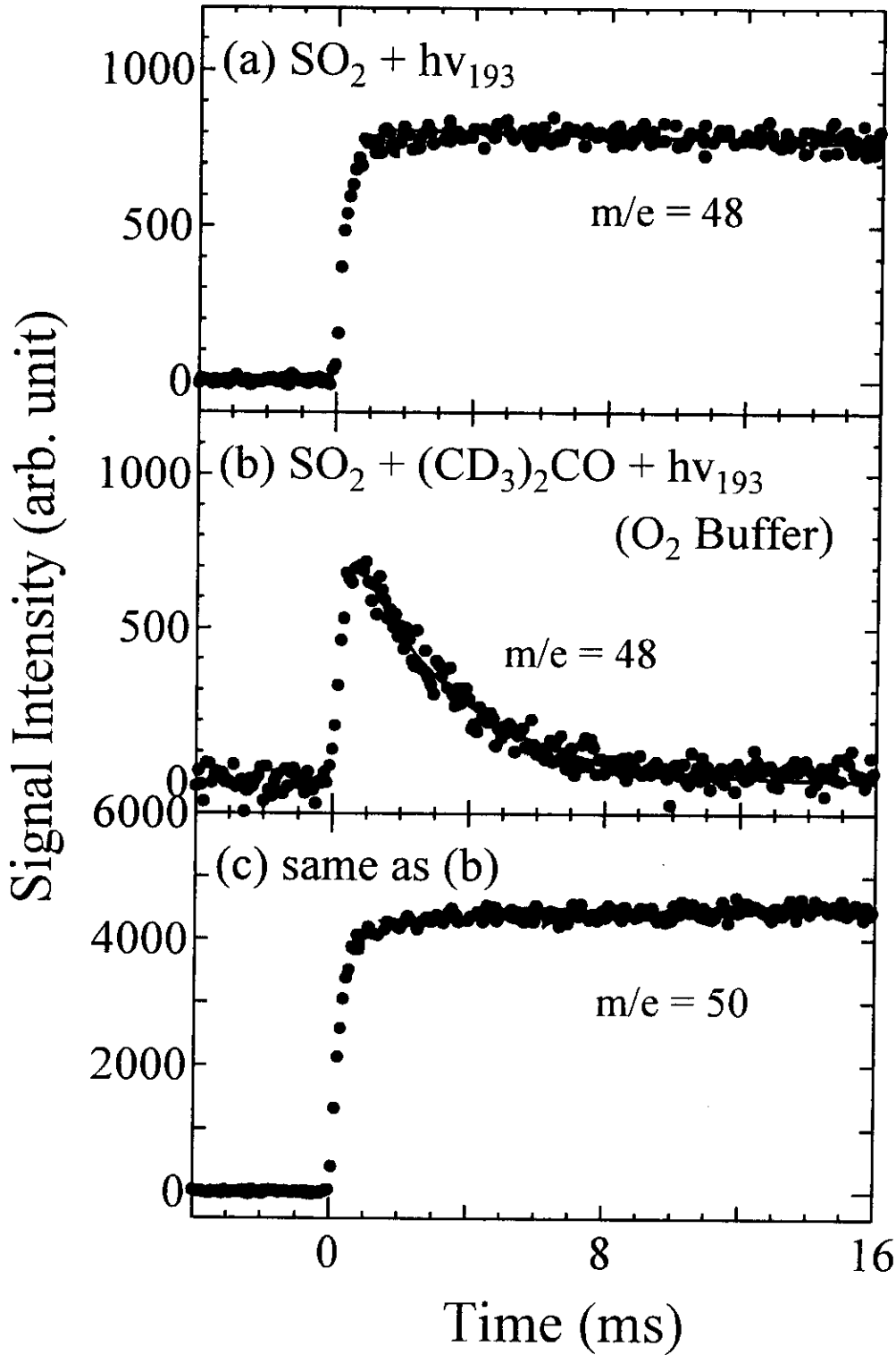

Figure 2. Time profiles of SO (a) in the absence of and (b) in the presence of CD_3O_2 radicals. (c) Time profile of CD_3O_2 during the measurement of the decay profile of SO shown in (b).

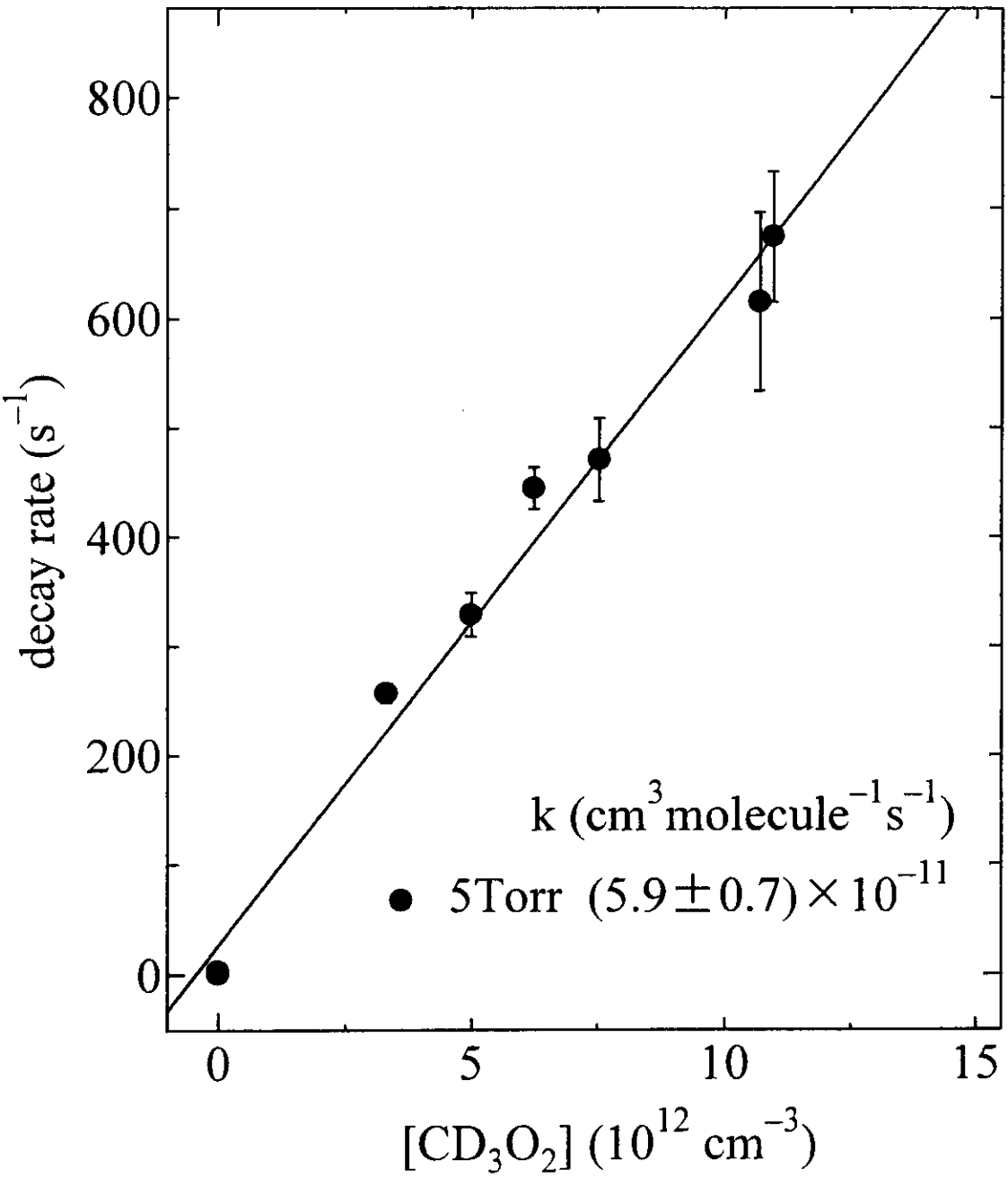

Figure 3. Plot of the first-order rate constant of SO against the concentration of CD_3O_2 radicals.

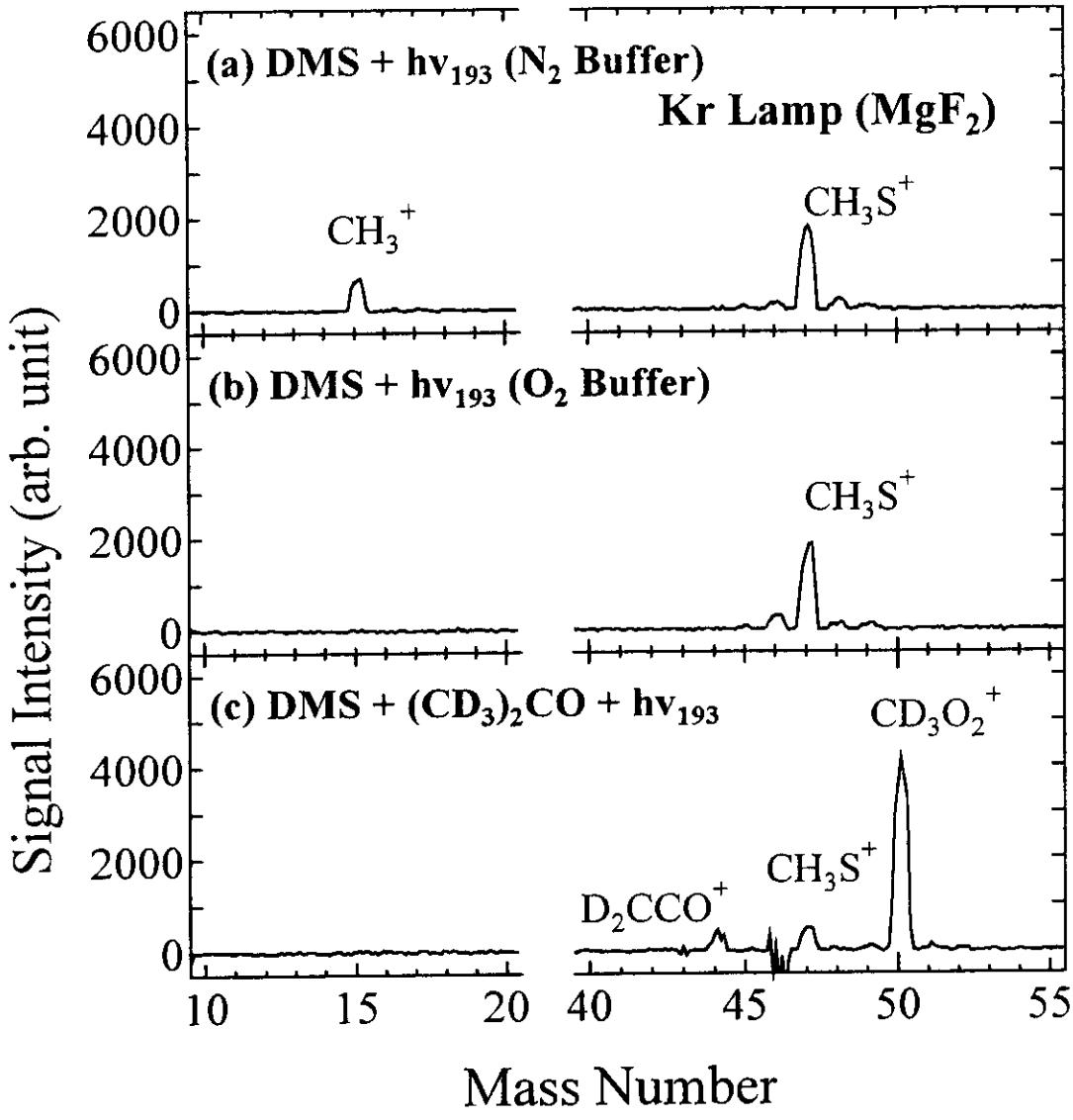

Figure 4. Time-resolved mass spectra taken in (a) DMS + $h\nu_{193nm}$ in N_2, (b) DMS + $h\nu_{193nm}$ in O_2, and (c) DMS + $(CD_3)_2CO$ + $h\nu_{193nm}$ in O_2 systems. The spectra were obtained by subtracting the ion signals taken for 2 ms before laser photolysis from those taken during 2-4 ms after photolysis.

Since the mass number of CH_3S is identical with CH_3O_2, we investigated the reaction of $CH_3S + CD_3O_2$ instead of $CH_3S+CH_3O_2$. When CD_3O_2 was produced, the decrease of the signal intensity of CH_3S was observed (Fig. 4c). This suggests the CH_3S can react with CD_3O_2.

The first-order rate constant of CH_3S , k_2', was obtained by fitting the decay profile using a single-exponential function. Since the concentration of CD_3O_2 was in the large excess over CH_3S radicals, k_2' should be represented by

$$k_2' = k_{2w}' + k_2 \times [CD_3O_2],$$

where k_{2w}' is the first-order rate constant taken in the absence of CD_3O_2 and k_2 is the second-order rate constant for reaction (2). Fig. 5 shows a plot of k_2' as a function of the concentration of CD_3O_2. The second-order rate constant for reaction (2) was determined to be 7.2×10^{-11} $cm^3molecule^{-1}s^{-1}$ from the slope of the figure.

2.3.3. $HS + CH_3O_2 \rightarrow HSO + CH_3O$ reaction

The rate constant for reaction (3), k_3, was also measured in a similar manner. Since the photolysis of acetone did not interfere the HS signal (m/e = 33), CH_3O_2 (generated from acetone-h_6) could be used for rate measurements. The rate constant was determined to be 1.1×10^{-10} $cm^3molecule^{-1}s^{-1}$.

3. Effects of temperature and NO_X concentration on SO_2 yield in the photooxidation of DMS

3.1. Introduction

Dimethyl sulfide (DMS) is the dominant biogenic sulfur compound and is mainly emitted from oceans. Its photooxidation is mainly initiated by reaction with OH radical, which leads to production of oxidized forms, i.e. SO_2, CH_3SO_3H, and H_2SO_4. Part of SO_2 is oxidized in the gas phase and converted to H_2SO_4, which plays a role as condensation nuclear. On the other hand, methane sulfonic acid (CH_3SO_3H, MSA) is believed to be taken up into particles already exist. Therefore, the production of SO_2 and H_2SO_4 from DMS should affect on the radiative forcing through the formation of sulfate aerosols, while MSA has only minor impact on forcing. An interesting hypothesis of a climate feedback loop involving DMS was proposed: increase of temperature → increase of DMS emissions → increase of sulfate concentration → increase of aerosol and cloud condensation nuclei concentrations → decrease of radiative forcing.[2] However, until now, the effect of temperature on the formation yield of SO_2 in the photooxidation of DMS has not yet been studied. In this work, we measured the SO_2 yield as a function of temperature as well as the NO_X concentration to understand the mechanism of photooxidation of DMS.

3.2. Experimental

A 6-m^3 bakable and evacuable photochemical reaction chamber was used for all of the experiments. Nineteen 1-kW Xe-arc lamps were used for photoirradiation. The concentration of the reactants and products were monitored by means of an FT-IR with a White cell system (optical path length = 221.5 m). The wall of the chamber was temperature-controlled (15 - 50 °C). The temperature in the chamber was monitored with a humidity and temperature transmitter. Methyl nitrite (CH_3ONO) was used as OH radical source for all of the experiments.

3.3. Results and discussion

The SO_2 formation yield, $Y_{SO2}(\%) = 100 \times \{[SO_2]_t / ([DMS]_0 - [DMS]_t)\}$, was

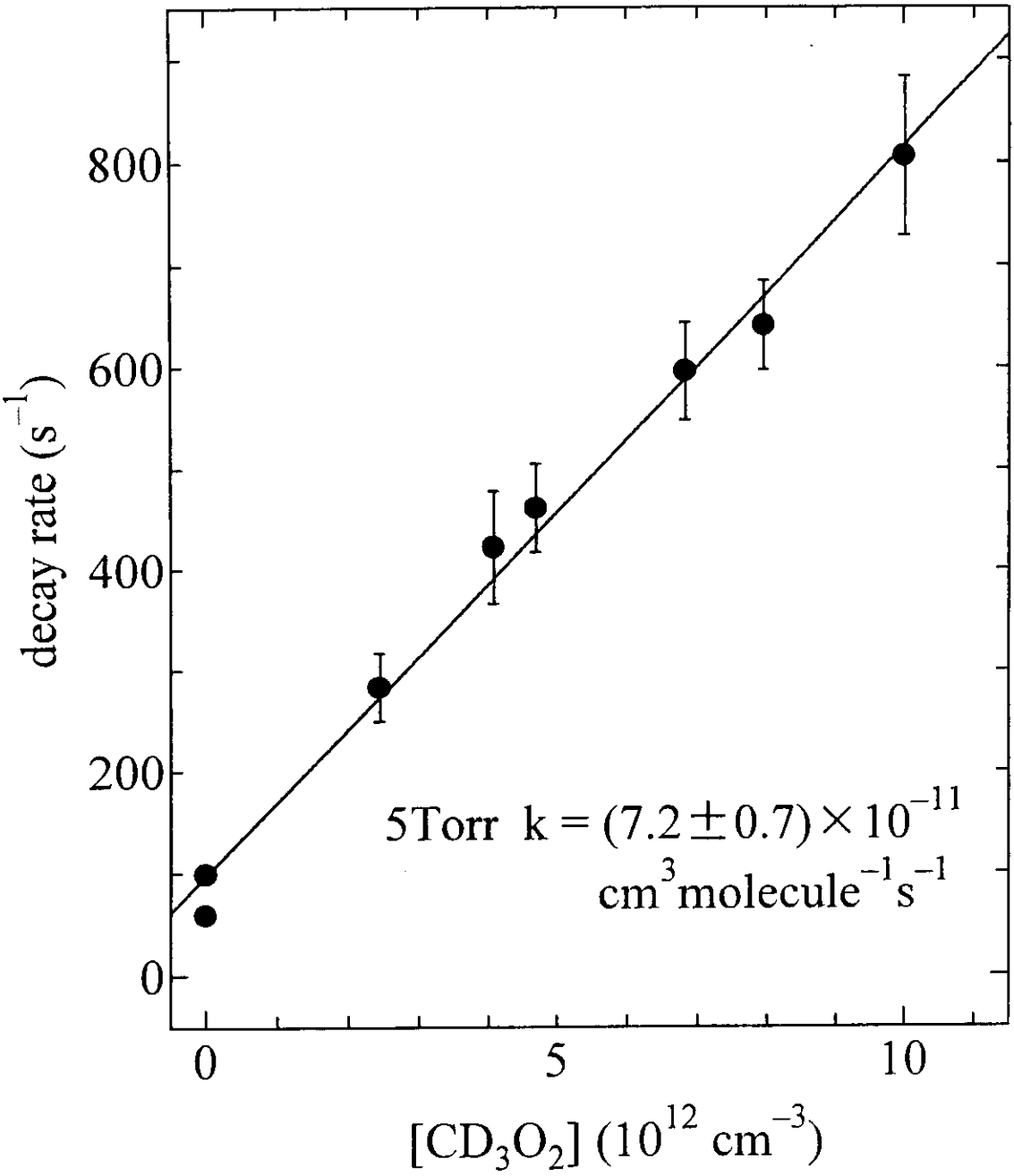

Figure 5. Plot of the first-order rate constant of CH_3S as a function of the concentration of CD_3O_2.

observed as a function of the percentage of DMS reacted, $R_{DMS}(\%) = 100 \times \{1 - [DMS]_t / [DMS]_0\}$, in a DMS(6ppm)-$CH_3ONO$(20ppb)-dry air-irradiation system at 15, 25 and 50 °C, and is shown in Fig.6. As shown in the figure, Y_{SO2} is sensitive to temperature but almost independent of R_{DMS}.

The SO_2 yield was also observed at 50 and 200 ppb of the initial concentration of CH_3ONO, $[CH_3ONO]_0$, and are plotted in Fig.7. It is clear that the SO_2 yield increases with decreasing $[CH_3ONO]_0$ and increases with increasing temperature under our experimental condition. Furthermore, the formation of MSA was observed when NO_X concentration increased.

The reaction of OH with DMS is believed to proceed by two channels, the abstraction and the addition channels:

$$OH + CH_3SCH_3 \rightarrow H_2O + CH_2SCH_3, \quad (10a)$$

$$OH + CH_3SCH_3 + M \rightarrow CH_3S(OH)CH_3 + M. \quad (10b)$$

The branching between two channels should vary as a function of temperature. However, the current recommended kinetic data for reaction (10) [3] suggest that the abstraction channel is dominant and its branching ratio, k_{10a}/k_{10}, is not sensitive to temperature in the range of 15-50 °C; i.e., k_{10a}/k_{10} 0.83 at 15°C and 0.84 at 50°C. Therefore, the temperature dependence on Y_{SO2} observed in this work could not be attributed to the branching in reaction (10).

One of possible processes to influence the SO_2 yield is the reactions of CH_3SO_2. CH_3SO_2 radicals have a number of fates, including decomposition to CH_3+SO_2 and reactions with NO_2, O_2, and O_3:

$$CH_3SO_2 + M \rightarrow CH_3 + SO_2 + M, \quad (11)$$

$$CH_3SO_2 + NO_2 \rightarrow CH_3SO_3 + NO, \quad (12)$$

$$CH_3SO_2 + O_2 + M \leftrightarrow CH_3SO_2O_2 + M, \quad (13,-13)$$

$$CH_3SO_2 + O_3 \rightarrow \text{products}. \quad (14)$$

The rate constants for these reactions at room temperature have been reported: $k_{11} = 510\ s^{-1}$ at 1 Torr [4] and $k_{12} = 2.2 \times 10^{-12}$,[4] $k_{13} < 6 \times 10^{-18}$,[5] and $k_{14} < 8 \times 10^{-13}$ [5] $cm^3molecule^{-1}s^{-1}$. As the temperature increases, the rate of the thermal decomposition will also increase. Since the rate constant for reaction (13) is small, the reproduction of CH_3SO_2 through reaction (-13) is expected to be important near room temperature. It was recently reported that the yield of MSA increased as the NO_X concentration increased.[6] This fact was also confirmed in this work. Furthermore, the production of $CH_3SO_2O_2NO_2$ in the presence of NO_X was also reported.[6] These results suggested that the peroxy radical produced by reaction (13) could react with NO_X:

$$CH_3SO_2O_2 + NO \rightarrow CH_3SO_3 + NO_2, \quad (15)$$

$$CH_3SO_2O_2 + HO_2 \rightarrow CH_3SO_3H\ (MSA) + O_2, \quad (16)$$

$$CH_3SO_2O_2 + NO_2 + M \rightarrow CH_3SO_2O_2NO_2 + M. \quad (17)$$

The observed dependence of temperature and the NO_X concentration could, at least qualitatively, explained in terms of the branching in CH_3SO_2 reactions as follows; It is expected that the rate of reaction (11) is depressed, the equilibrium in reaction (13, -13) is shifted toward right, and the rates of reactions (15) and (17) are enhanced when the temperature is low and the NO_X concentration is high. These lead to a decline of the SO_2 yield. On the other hand, under high temperature and low NO_X concentration conditions, it appears that the rate of reaction (11) is enhanced but the rates of reactions (15) and (17) are reduced, and the equilibrium in reaction (13, -13) is shifted toward left. Hence the SO_2 yield is

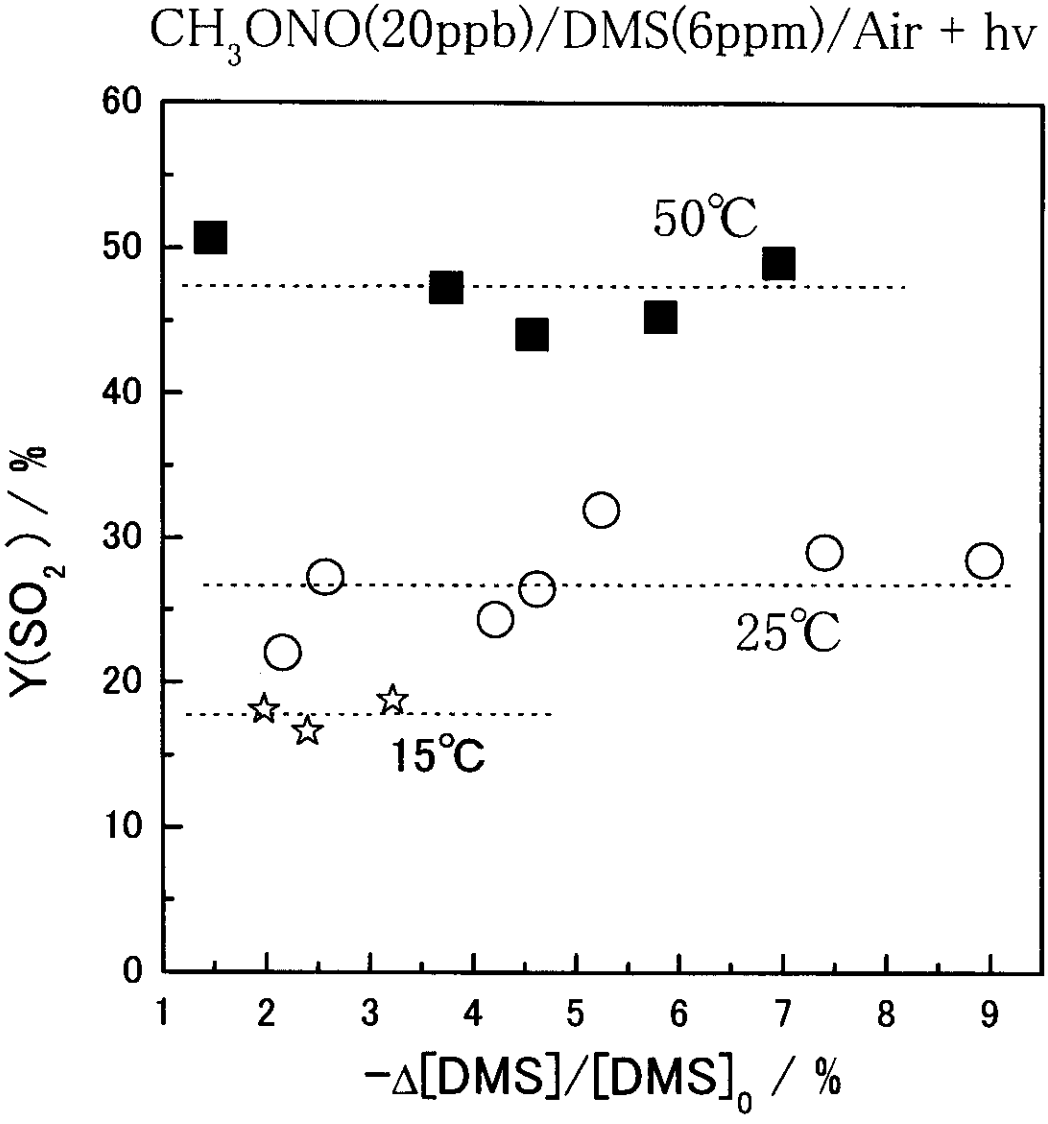

Figure. 6. Plots of the SO_2 yields obtained as a function of the percentage of fate of CH_3SCH_3.

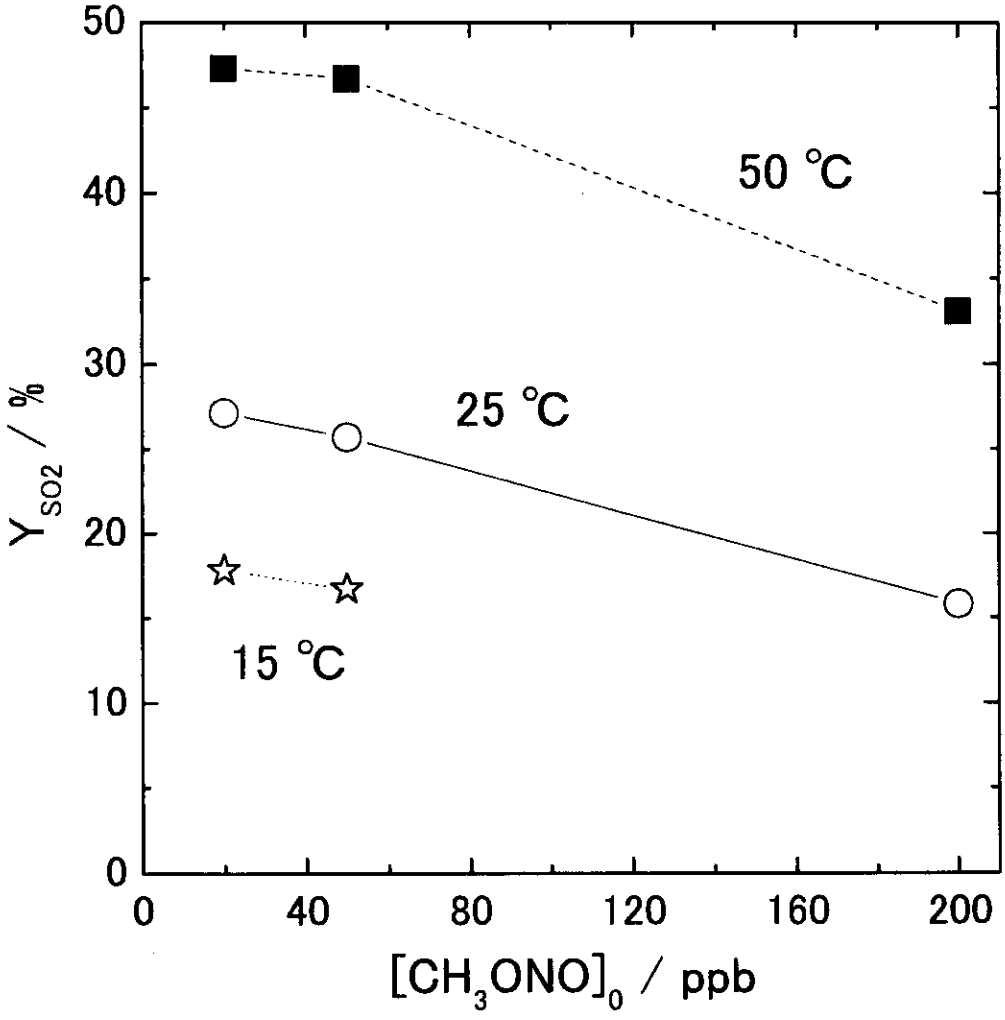

Figure. 7. Plots of SO_2 yield as a function of the initial concentration of CH_3ONO.

enhanced.

References

[1] IPCC (1996), "*Climate Change 1995: The Science of Climate Change*", J. T. Houghton et al., eds., Intergovernmental Panel on Climate Change, Cambridge University Press, Cambridge, UK.

[2] R. J. Charlson et al. (1987), *Nature,* **326**, 655.

[3] W. B. DeMore et al. (1997), "*Chemical Kinetics and Photochemical Data for Use in Stratospheric Modeling*", JPL, Caltech, Evaluation No. 12, JPL Publ. 97-4.

[4] A. A. Turnipseed and R. A. Ravishankara (1993), "*Dimethylsulfide: Oceans, Atmosphere, and Climate*", G. Restelli and G. Angeletti, eds., Kluwer Academic, Dordrecht/Norwell, MA

[5] A. Ray et al. (1996), *J. Phys. Chem.*, **100**, 8895.

[6] I. V. Patroescu et al. (1999), *Atmos. Environ.*, 33, 25.